Biochemical purification uncovers mammalian sterile 3 (MST3) as a new protein kinase for multifunctional protein kinases AMPK and SIK3

Received for publication, February 28, 2022, and in revised form, March 30, 2022 Published, Papers in Press, April 10, 2022,
https://doi.org/10.1016/j.jbc.2022.101929

Yuxiang Liu[1,2,3,4], **Tao V. Wang**[1,2,3,4], **Yunfeng Cui**[1,2,3,4], **Shengxian Gao**[1,2,3,4], **and Yi Rao**[1,2,3,4,*]

From the [1]*Laboratory of Neurochemical Biology, Department of Chemical Biology, College of Chemistry and Chemical Engineering, PKU-IDG/McGovern Institute for Brain Research, Peking-Tsinghua Center for Life Sciences, School of Life Sciences, School of Pharmaceutical Sciences, Health Sciences Center, Peking University, Beijing, China;* [2]*Chinese Institute for Brain Research, Beijing, China;* [3]*School of Basic Medical Sciences, Capital Medical University, Beijing, China;* [4]*Changping Laboratory, Beijing, China*

Edited by Henrik Dohlman

The AMP-activated protein kinase (AMPK) and AMPK-related kinase salt-inducible kinase 3 (SIK3) regulate many important biological processes ranging from metabolism to sleep. Liver kinase B1 is known to phosphorylate and activate both AMPK and SIK3, but the existence of other upstream kinases was unclear. In this study, we detected liver kinase B1–independent AMPK-related kinase phosphorylation activities in human embryonic kidney cells as well as in mouse brains. Biochemical purification of this phosphorylation activity uncovered mammalian sterile 20–like kinase 3 (MST3). We demonstrate that MST3 from human embryonic kidney cells could phosphorylate AMPK and SIK3 *in vivo*. In addition, recombinant MST3 expressed in and purified from *Escherichia coli* could directly phosphorylate AMPK and SIK3 *in vitro*. Moreover, four other members of the MST kinase family could also phosphorylate AMPK or SIK3. Our results have revealed new kinases able to phosphorylate and activate AMPK and SIK3.

Protein kinases play crucial roles in biological processes and diseases. Nearly half a century ago (1–8), the activities of what is later known as the AMP-activated protein kinase (AMPK) were detected. AMPK is a highly conserved eukaryotic kinase capable of sensing AMP/ATP ratio and regulating energy homeostasis (9–12). It can also sense inositol (13) and plays multiple crucial roles ranging from energy balance to autophagy. AMPK is a therapeutic target for diseases ranging from metabolic disorders to tumors (14–17).

Mammalian AMPK exists as a heterotrimeric complex, formed by α, β, and γ subunits (18–20). There are 12 possible combinations of the αβγ trimer from one each of the two α subunits, two β subunits, and three γ subunits (21–28). The α subunit is catalytic, and its activity is regulated by phosphorylation at threonine 172 (T172) of AMPKα2 or its equivalent T183 in AMPKα1 (29).

The liver kinase B1 (LKB1), whose gene is mutated in human Peutz–Jeghers syndrome (30), was found to phosphorylate AMPKα2 at T172 or AMPKα1 at T183 (31–38). The Ca^{2+}/calmodulin-dependent protein kinase kinase 2 (CaMKK2, also known as CaMKKβ) can also phosphorylate AMPKα-T172 (39–42). Transforming growth factor-β–activated kinase-1 (also known as mitogen-activated protein kinase kinase kinase 7) was reported to phosphorylate AMPKα2 at T172 (43–45), though it is not accepted as widely as LKB1 or CaMKK2 (46) as an AMPK.

There are 14 AMPK-related kinases (ARKs) (36), of which the salt-inducible kinase 3 (SIK3) has been found to be an important regulator of sleep (47). PKA can phosphorylate several sites in SIK3, and their significance in sleep regulation has been demonstrated previously (47, 48). The biochemical significance of threonine 221 (T221) in SIK3 activity and stability as well as the physiological significance of SIK3-T221 in sleep need have been discovered by us recently (49). LKB1 and its associated proteins STRAD and MO25, when immunoprecipitated from human embryonic kidney (HEK) 293 cells, could potently phosphorylate T221 of SIK3 and increase its activity (36). It was reported that CaMKK2 could only phosphorylate AMPKα-T172 but not SIK3-T221 or equivalent sites in other ARKs (50).

During our studies of SIK3 phosphorylation, we obtained evidence that SIK3-T221 could be phosphorylated by activities independent of LKB1 in HEK cells and mouse brains. We carried out biochemical purification with 50 l of HEK cells cultured in suspension and approximately 5000 mg proteins of HEK lysates. Our purification uncovered mammalian sterile 20–like (MST) kinase 3 (MST3) (51–53). We then tested and found that MST 1, 2, 3, 4, and 5 could phosphorylate SIK3-T221 and AMPKα-T172. MSTs are thus new kinases for AMPK and SIK3.

Results and discussion

Detection of LKB1-independent SIK3-T221 phosphorylation activities in mouse brains and HEK cells

To find a standard SIK3 substrate, we transfected complementary DNAs (cDNAs) encoding different fragments of the SIK3 protein into HEK cells and tested them for

* For correspondence: Yi Rao, yrao@pku.edu.cn.

phosphorylation at T221, which was detected by immunoblot analysis with a phosphospecific antibody (49). We found that fragments containing amino acid residues 59 to 558, 59 to 658, and 59 to 758 were good substrates, whereas those containing amino acids 59 to 385, 59 to 458, 59 to 858, and 59 to 958 were not (Fig. S1). We thereafter expressed SIK3 59 to 558 in *Escherichia coli* and used it as the standard substrate in our assays for SIK3-T221 phosphorylation.

Extracts were made from either HEK293T cells or mouse brains and fractionated on different chromatography columns before different fractions were tested for SIK3-T221 phosphorylation (Figure 1*A*). Briefly, brains from 10 C57 mice of 8 weeks old were extracted, and each brain was lysed in 4 ml of lysis buffer, ground in tissue homogenizer for 240 s, and centrifuged for 20 min at 14,000 rpm. Supernatants were collected and filtered at 0.45 μm. Protein concentrations were measured, and aliquots were made. For HEK293T cells, 30 culture dishes (of 100 mm, in diameter) (1.0–1.5 × 10^7 cells/dish) were lysed and homogenized for 240 s, centrifuged at 14,000 rpm for 20 min, and filtered at 0.45 μm. Proteins were measured for concentration and aliquoted.

Purification was carried out at 4 °C with an AKTA Purifier10 FPLC system (GE Healthcare). Cell lysates were loaded onto an anionic exchange (Q sepharose high performance column [Q HP]) column of 1 ml bead volume pre-equilibrated with buffer A, and flow-through lysates were collected approximately one column bed volume (1 ml/fraction). We used one column volume (CV) per fraction as the standard fraction in our purification. The column was washed with 5 CV buffer A (20 mM Hepes,10 mM KCl, 1.5 mM $MgCl_2$, 1 mM EDTA, 1 mM EGTA, 1 mM DTT, 1× protease inhibitor cocktail, 1× phosphatase inhibitor II, and 1× phosphatase inhibitor III) until baseline and conductivity were stable. The column was eluted with a linear gradient of 20 CV (fractions 1–20) from 0 to 600 mM sodium chloride (NaCl) and step gradient elution of 5 CV (fractions 21–25) from 600 to 1000 mM NaCl. Fractions were collected 1 CV (1 ml) of the eluent, and aliquots of 0.5 ml of each fraction were dialyzed against buffer A, and 10 μl fractions were incubated with 1 μg recombinant SIK3 amino acids 59 to 558 at 37 °C for 1 h in buffer A with a final concentration of 1 mM ATP (pH 7.5) in a total volume of 20 μl. The reaction was terminated by heating at 95 °C with the protein loading buffer and analyzed by immunoblotting. Flow-through fractions 2 to 3 (0 mM NaCl), fractions 4 to 7 (90–180 mM NaCl), and fractions 15 to 20 (420–570 mM NaCl) of mouse brain extracts were found to contain strong (in fractions 5–7, 120–180 mM NaCl) or weak (in flow-through fractions 2 and 3) activities in phosphorylating the recombinant SIK3 at T221. Fractions 15 to 20 displayed weak phosphorylating activity. LKB1 was detected in fractions 12 to 14 (330–390 mM NaCl) strongly but weakly in fractions 15 to 21 (420–600 mM NaCl). It was not possible to attribute the activities in fractions 5 to 7 to LKB1 (Fig. 1*B*).

Fractionation of HEK extracts was carried out similarly as the fractionation of mouse brain lysates described previously. Of the fractions collected from the Q column of HEK extracts (Fig. 1*C*), flow-through fractions 2 and 3 (0 mM NaCl) and fractions 4 and 5 (90–120 mM NaCl) contained strong and fractions 12 to 16 (330–450 mM NaCl) had moderate SIK3-T221 phosphorylation activities. LKB1 was detected in fractions 11 to 13 (300–360 mM NaCl) but could not explain the activities in flow-through fractions 2 and 3 or fractions 4 and 5 (Fig. 1*C*).

HEK cell lysates were loaded onto a cationic exchange column (SP sepharose high performance column [SP HP]) of 10 ml bead volume, and flow-through lysates were collected one column bed volume (10 ml/fraction). The column was eluted with a linear gradient of 20 CVs from 0 to 600 mM NaCl and step gradient elution of 5 CVs from 600 to 1000 mM NaCl gradient elution. About 10 μl fractions were tested for kinase activities after dialysis. Fractions 7 (180 mM NaCl) and 12 (330 mM NaCl) phosphorylated SIK3-T221 strongly, but LKB1 was detected strongly in fractions 4 to 6 (90–150 mM NaCl) and weakly in fractions 7 to 9 (180–240 mM NaCl; Fig. 1*D*).

HEK cell lysates were subjected to the Superdex 75 10/300 GL size-exclusion column (24 ml bed volume) and eluted with 200 mM NaCl in buffer A. The eluted fractions were collected 1 ml/fraction from 0 to 24 ml, and 10 μl fractions were tested for kinase activities after dialysis. Fractions 12, 13, and 14 (330–420 mM NaCl) phosphorylated SIK3-T221, with the strongest activity in fraction 13 (360 mM NaCl) and moderate activities in fractions 12 (330 mM NaCl) and 14 (390 mM NaCl). But LKB1 was detected strongly in fractions 10 and 11 (270–300 mM NaCl), moderately in fraction 12 (330 mM NaCl), not in fractions 13 and 14 (330–420 mM NaCl; Fig. 1*E*).

HEK cell extracts were fractionated on a 1 ml heparin column. Fractions 11 to 14 (300–420 mM NaCl) had the strongest SIK3-T221 phosphorylating activity, with moderate activities in fractions 9 and 10 (240–270 mM NaCl), weak activities in fractions 8 (210 mM NaCl) and 15 (420 mM NaCl), whereas LKB1 was strongly detected in fractions 20 and 21 (570–600 mM NaCl) and weakly in fractions 16 to 19 (450–570 mM NaCl; Fig. 1*F*).

Thus, fractionations of both mouse brains and HEK cell extracts indicate that there were fractions with strong SIK3-T221 phosphorylating activities but no LKB1, suggesting the possible existence of LKB1-independent activities that can phosphorylate T221 of SIK3.

Purification of MST3 as a candidate kinase phosphorylating SIK3-T221

We tested six different chromatography columns before designing a purification scheme illustrated in Figure 2*A*.

About 50 l of HEK293T cells cultured in suspension at a density of 3 × 10^6 cells/ml were collected, and cell pellets were diluted in lysis buffer before grinding and centrifugation. Cell lysates containing a total of 5000 mg (at 10 mg/ml) protein were used for purification. About 500 mg was filtered at 0.45 μm and fractionated by a 10 ml SP HP column and eluted with NaCl gradient (0–600 mM) into 20 fractions, followed by 1 M NaCl washing of 5 CV. Each fraction was examined for SIK3-T221 phosphorylating activity. Similar to results shown

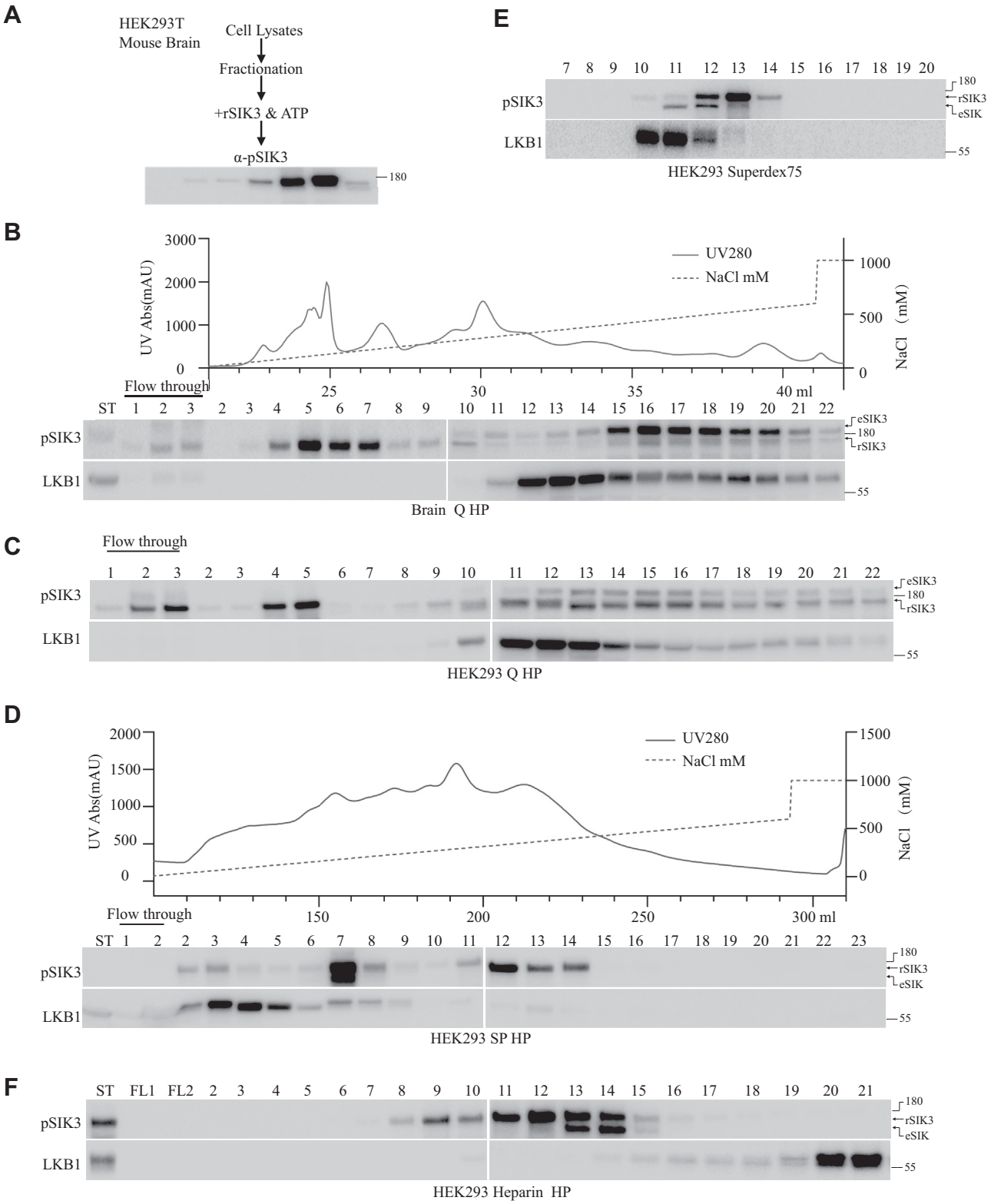

Figure 1. SIK3-T221 phosphorylation by extracts from mouse brains and HEK cells. *A*, a diagram for detection of SIK3-T221 phosphorylating activities in fractions of HEK293 cells and mouse brain extracts. Each fraction was individually tested with the recombinant SIK3 (rSIK3) substrate (Fig. S1*A*) in the presence of ATP. Because the substrate is a recombinant protein made from *Escherichia coli* (Fig. S1*A*), the amount used for each phosphorylating assay was the same and thus not shown. An example of results from anti-SIK3 phospho-T221 antibody analysis is shown at the *bottom*. *B*, SIK3-T221 phosphorylating activities in the mouse brain. *Upper panel* shows protein absorbance at 280 nm and NaCl gradient, whereas *lower panels* show SIK3 T221 phosphorylating activities and LKB1. Extracts were made from 10 brains of C57 mice at 8 weeks of age, each brain lysed with 4 ml of cell lysis buffer in cold, ground for 240 s, and centrifuged for 20 min at 14,000 rpm. Supernatants were collected and filtered through a 0.45 μm filter. Lysates with 50 mg of proteins (at a concentration of 10 mg/ml) were fractionated on an anionic Q HP column and eluted with a gradient of NaCl (*upper panel*). The *lower panels* show SIK3-T221 phosphorylating activities and detection of LKB1 by immunoblot analysis. The flow-through fractions 2 and 3 (0 mM NaCl) showed weak SIK3-T221 phosphorylating activity. Fractions 5 to 7 (120–180 mM NaCl) showed strong activities. rSIK3 indicates the recombinant SIK3, whereas eSIK3 indicates SIK3

in Figure 1*D*, fraction 7 (180 mM NaCl) had the highest activity (Fig. 2*A*). The rest of the HEK cell lysates, 500 mg each, were also fractionated by the SP HP column.

Active fractions from the SP HP column were then combined. About 10% of the total was fractionated sequentially on 10 ml heparin HP, 10 ml Q HP, 1 ml hydroxyapatite (HAP), Superdex 75 10/300 GL, and 1 ml Mono S columns (Figs. 2 and 3*A*). Each round fractionation was examined for SIK3-T221 phosphorylating activities (Fig. 2, *A–E*). The behavior of the large preparation from the 50 l of HEK cells upon fractionation was slightly different from that of the smaller preparation from 30 dishes of HEK cells. After reexamination, we went through the purification with extracts from all 50 l of HEK cells, with fractions predicted from the results of the 10% initial run. Each of the 20 fractions from the last column (Mono S) was examined for SIK3-T221 phosphorylation and silver stained for proteins (Fig. 3*B*).

SIK3-T221 phosphorylating activity was strongly detected in fraction 8 (210 mM NaCl) and moderately in fraction 9 (240 mM NaCl) of our last (Mono S) column (Fig. 3*B*). We cut multiple bands from fraction 8 (indicated as bands 1, 2, 4, and 5 in Fig. 3*B*) and fraction 9 (bands 3 and 6 in Fig. 3*B*). They were subjected to mass spectrometry analysis.

Six kinases were detected in these bands by mass spectrometry (Fig. 3*C*). One was a pantothenate kinase 1, and five were protein kinases (MST3, MST4, STK39, FES, and ADCK2). MST3, MST4, and STK39 were serine/threonine kinases, FES a tyrosine kinase, and ADCK2 an uncharacterized kinase (Fig. 3*C*).

Confirmation of MST3 as a kinase phosphorylating SIK3-T221 in vivo

We expressed LKB1, GFP, and each of the six kinases as a FLAG-tagged protein in HEK293 cells. We immunoprecipitated each of them with the anti-FLAG antibody and tested them on the recombinant SIK3 substrate in the presence of ATP. GFP could not phosphorylate SIK3-T221, but LKB1 could phosphorylate SIK3-T221 (Fig. 3*D*). SIK3-T221 could be phosphorylated by either MST3 or MST4 but none of the other four kinases (STK39, FES, ADCK2, and pantothenate kinase 1) (Fig. 3*D*).

MST3 is a member of the STE20-like kinases including MSTs 1 to 5 (51–53). Mutation of lysine (K) 53 to arginine (R) in MST3 led to a kinase-dead mutant, mutation of T178 to alanine (A) reduced its activity, whereas T178 mutation to glutamic acid (E) resulted in a constitutively active kinase (52, 54). Similar to the SIK3 WT substrate, we also expressed its mutant form SIK3 T221A in *E. coli*. We found that FLAG-tagged MST3 WT immunoprecipitated from HEK cells phosphorylated SIK3 WT but not SIK3 T221A (Fig. 3*E*). MST3 carrying the T178A mutation phosphorylated neither SIK3 WT nor SIK3 T221A. MST3 carrying the T178E mutation phosphorylated SIK3 WT not SIK3 T221A, though to a lesser extent than MST3 WT. MST3 K53R could not phosphorylate SIK3 WT or SIK3 T221A (Fig. 3*E*).

In HEK cells, increasing amounts of cDNAs expressing MST3 WT or MST3 T178E led to increased phosphorylation of SIK3-T221 (Fig. 3*F*). Increasing amounts of MST3 WT and MST3 T178E also increased SIK1 phosphorylation in HEK cells (Fig. S2*A*). FLAG-tagged MST3 WT immunoprecipitated from HEK cells phosphorylated recombinant SIK1 at T182 (Figs. S1*B* and S2*B*) and recombinant SIK2 at T175 (Figs. S1*C* and S2*C*). MST3 carrying the T178A mutation phosphorylated neither SIK1-T182 nor SIK2-T175. MST3 carrying the T178E mutation phosphorylated SIK1-T182 and SIK2-T175, though to a lesser extent than MST3 WT. MST3 K53R could not phosphorylate SIK1-T182 (Fig. S2*B*) or SIK2-T175 (Fig. S2*C*).

These results indicate that MST3 is a kinase for the activation loop T in SIK1, SIK2, and SIK3.

Direct phosphorylation of SIK3-T221 by recombinant MSTs in vitro

Experiments described previously were performed with HEK cells *in vivo*. To investigate whether MSTs directly phosphorylate SIK3-T221 and enhance the catalytic function of SIK3, we expressed recombinant forms of all proteins in

endogenous to HEK cells. The rSIK3 used as the substrate here was made in *E. coli* and fused as MBP-TEV-3x FLAG-SIK3 59-558-TEV-GFP-8xHis tag (Fig. S7 in the companion article) and thus only slightly smaller than the eSIK3 in HEK cells. Fractions 15 to 20 (420–570 mM NaCl) showed strong phosphorylation of eSIK3 and weak phosphorylation of rSIK3. The strongest signals detected with an anti-LKB1 antibody were in fractions 12 to 14 (330–390 mM NaCl) and moderate signals in fractions 15 to 21 (420–600 mM NaCl). *C*, SIK3-T221 phosphorylating activities in HEK cells. Extracts were prepared from 30 dishes of 100 mm (at a cell confluence of 1.0–1.5 × 10^7 cells/dish). Lysates with 30 mg proteins (in a concentration of 2 mg/ml) were filtered at 0.45 μm and fractionated on a Q HP column and eluted with NaCl. Strong SIK3-T221 phosphorylating activities were detected in flow-through fractions 2 and 3 (0 mM NaCl), and fractions 4 and 5 (90–120 mM NaCl), with moderate activities in fractions 12 to 16 (330–450 mM NaCl). LKB1 was detected in fractions 11 to 13 (300–360 mM NaCl) strongly and fractions 14 to 16 (390–450 mM NaCl) moderately. rSIK3 indicates the rSIK3, whereas eSIK3 indicates SIK3 endogenous to HEK cells. *D*, *upper panel* shows protein absorbance at 280 nm and NaCl gradient, whereas *lower panels* show SIK3-T221 phosphorylating activities and LKB1. HEK cell lysates with 500 mg proteins (in a concentration of 10 mg/ml) were filtered at 0.45 μm and fractionated through an SP HP column. rSIK3 is the *upper band* in the *upper panel*. The *lower band* in the *upper panel* is an eSIK (cf., analysis in Fig. S1*D*). SIK3-T221 phosphorylating activities were strongly detected in fractions 7 (180 mM NaCl) and 12 (210 mM NaCl), moderately in fractions 2 and 3 (30–60 mM NaCl), and fractions 8 (210 mM NaCl), 11 (300 mM NaCl), 13 (360 mM NaCl), and 14 (390 mM NaCl). LKB1 was detected strongly in fractions 4 to 6 (120–180 mM NaCl) and weakly in fractions 7 to 9 (21–270 mM NaCl). *E*, HEK cell lysates with 10 mg proteins (in a concentration of 20 mg/ml) filtered at 0.45 μm were fractionated on a Superdex 75 size-exclusion column. rSIK3 is the *upper band* in the *upper panel*. The *lower band* in the *upper panel* is an eSIK (cf., analysis in Fig. S1). Phosphorylation of the rSIK3 served as the indicator for the activity under purification. SIK3-T221 phosphorylating activities were strongly detected in fraction 13 (360 mM NaCl) and moderately in fractions 12 (330 mM NaCl) and 14 (390 mM NaCl). LKB1 was strongly detected in fractions 10 (270 mM NaCl) and 11 (300 mM NaCl) and weakly in fraction 12 (330 mM NaCl). *F*, HEK cell lysates with 30 mg proteins (in a concentration of 2 mg/ml) filtered at 0.45 μm were fractionated on a heparin HP column. The *upper band* in pSIK3 is the rSIK3, and the *lower band* is an eSIK. SIK3 T221 phosphorylating activities were strongly detected in fractions 11 to 14 (300–390 mM NaCl), moderately in the starting materials (ST) and fractions 9 (240 mM NaCl) and 10 (270 mM NaCl), and weakly in fractions 8 (210 mM NaCl) and 15 (420 mM NaCl). LKB1 was strongly detected in ST, fractions 20 (570 mM NaCl) and 21 (600 mM NaCl), and weakly in fractions 16 to 19 (450–570 mM NaCl). HEK, human embryonic kidney cell; LKB1, liver kinase B1; SIK3, salt-inducible kinase 3; T221, threonine 221; TEV, tobacco etch virus.

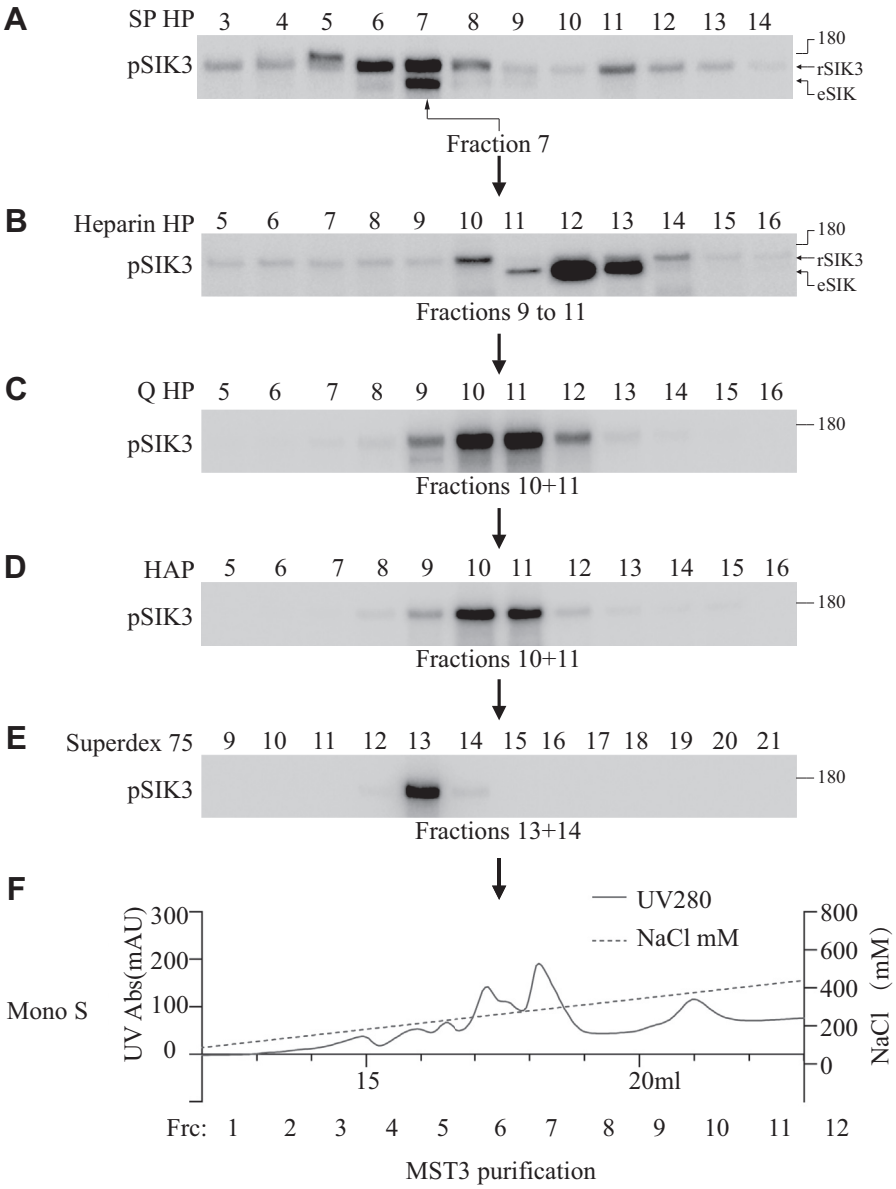

Figure 2. Purification of SIK3-T221 phosphorylating activities from HEK293T lysates. HEK cell lysates were purified in six sequentially connected chromatography steps in the order of SP HP, heparin HP, Q HP, HAP, Superdex 75, and Mono S. SIK3 T221 phosphorylating was monitored in each fraction from every column. Active fractions from each column were pooled and loaded onto the next column: fractions 9 to 11 (240–300 mM NaCl) from the heparin column, fractions 10 and 11 (370–300 mM NaCl) from the Q HP column, fractions 10 and 11 (270–300 mM NaCl) from the HAP column, and fractions 13 and 14 (200 mM NaCl) from the Superdex 75 column. We did not use fractions 12 and 13 (330–360 mM NaCl) from the heparin column because the strong bands in fractions 12 and 13 were smaller than the recombinant SIK3 band and were likely to be the endogenous phospho-SIK. Fractions from Mono S 5/50 GL column (shown in Fig. 2*B*) were dialyzed against buffer A and assayed for phosphorylation and used in silver staining. HEK293T, human embryonic kidney 293T cell; SIK3, salt-inducible kinase 3; T221, threonine 221.

E. coli. Recombinant kinases (0.5 μg each) were incubated with 1 μg recombinant SIK3 at 37 °C for 1 h in buffer A with a final concentration of 1 mM ATP (pH 7.5) in a total volume of 20 μl. The results were analyzed by immunoblotting with phosphospecific antibodies.

Recombinant human MST3 phosphorylated T221 in recombinant human SIK3 WT but not recombinant SIK3 T221A or T221E mutants (Fig. 4*A*). MST3b is an isoform of MST3 specifically expressed in the brain (55), and recombinant MST3b also phosphorylated recombinant SIK3 WT but not SIK3 T221A or T221E (Fig. 4*B*). Recombinant mouse MST3 phosphorylated recombinant SIK3 WT but not SIK3 T221A or T221E (Fig. 4*C*). These results have shown that recombinant MST3 directly phosphorylates recombinant SIK3-T221.

To investigate whether MST3 regulates the catalytic activity of SIK3, we generated recombinant human histone deacetylase 4 (HDAC4), which is a known substrate of SIK3 (56–58). With recombinant SIK3 and MST3, we found that MST3 increased the phosphorylation of HDAC4 by SIK3 (Fig. 4*D*).

To investigate the enzymatic kinetics of MST3, we measured the Michaelis–Menten constant of MTS3 by using the same concentration of recombinant MST3 with increasing concentrations of the recombinant SIK3 substrate (Fig. 4*E*). Kinase activities were analyzed by immunoblotting, and results

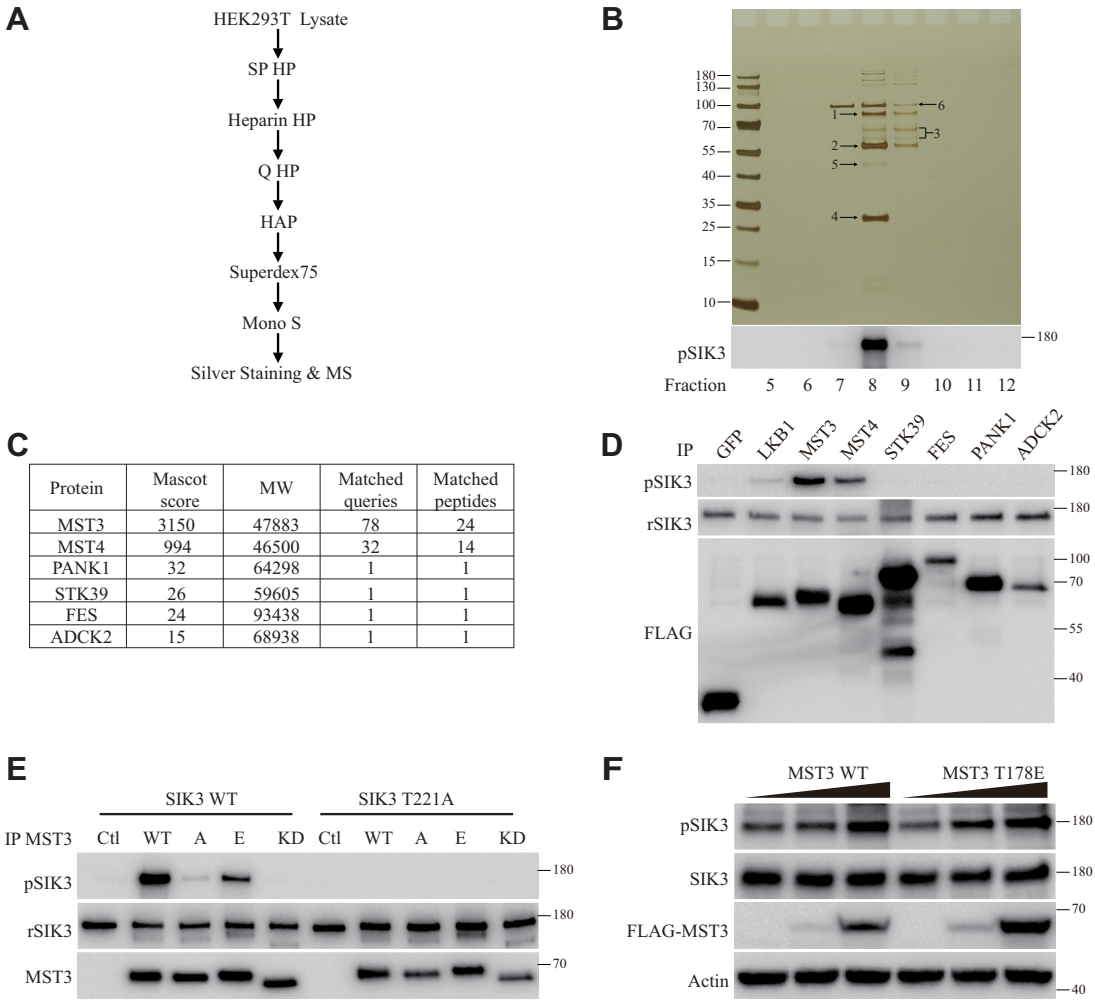

Figure 3. Purification and confirmation of MST3 as a SIK3-T221 kinase. *A*, a diagram for SIK3-T221 kinase purification. About 50 l of HEK cells cultured in suspension were used as the starting material, and six chromatographic columns were tested with a 10% equivalent of the starting material for purification of the activity before all materials were used. *B*, silver staining and SIK3-T221 phosphorylation assay of the fractions from the final column used in purification. Fractions from Mono S 5/50 GL column were dialyzed in buffer A and followed by *in vitro* SIK3 phosphorylation assay and silver staining. Strong phosphorylating activity was detected in fraction 8 (210 mM NaCl) and moderate activity in fraction 9 (240 mM NaCl). *Numbered arrows* point to bands isolated for MS. *C*, kinases identified by MS. MW, molecular weight (daltons). MST3, MST4, and STK39 are serine/threonine kinases, FES a tyrosine kinase, and ADCK2 a putative protein kinase. PANK1 is pantothenate kinase 1, phosphorylating pantothenate to 4′-phosphopantothenate. *D*, SIK3-T221 kinase activities of proteins expressed in HEK cells. cDNAs encoding FLAG-tagged kinases were transfected into HEK293T cells. Each was immunoprecipitated and assayed with the standard SIK3 substrate. *Bottom panel* shows FLAG recognized by its antibody, and top Western analysis with the anti–phospho-T221 antibody, *middle panel* the recombinant SIK3 substrate. SIK3-T221 was phosphorylated strongly by MST3 and MST4, weakly by LKB1, not by STK39, FES, ADCK2, or PANK1. *E*, the standard SIK3 WT substrate and its mutant form (T221A) were used to test the activities of different forms of MST3 expressed in and immunoprecipitated from HEK293T cells. MST3 WT and MST3 T178E (*E*) could phosphorylate SIK3 WT but not SIK3 T221A. MST3 T178A (*A*) and MST3 K53R (KD) could not phosphorylate SIK3 WT or SIK3 T221A. *pSIK3 panel* shows results of anti–phospho-SIK3-T221, *rSIK3 panel* the recombinant substrates, and *MST3 panel* MST3 WT and its mutants. *F*, MST3 enhanced SIK3-T221 phosphorylation *in vivo*. HEK293T cells were transfected with different concentrations of plasmids expressing FLAG-tagged MST3 WT or MST3 T178E and cultured for 24 h. Cells were treated with 200 nM okadaic acid (OA) for 1 h before lysis and Western analysis. Endogenous SIK3 (*second panel*) and its phosphorylation (*top panel*) were detected by anti-SIK3 and anti–phospho-T221 antibodies, respectively. Expression levels of FLAG-tagged MST3 or its mutant T178E were shown in the *third panel*. cDNA, complementary DNA; HEK, human embryonic kidney cell; MS, mass spectrometry; MST3, mammalian sterile 20–like kinase 3; SIK3, salt-inducible kinase 3; T221, threonine 221.

were quantitated with ImageJ software (National Institutes of Health). The Michaelis–Menten constant of MST3 on SIK3-T221 was calculated to be 7.59 μM by the GraphPad software (GraphPad Software, Inc).

Recombinant MST3 also increased the catalytic activities of recombinant SIK1 (Fig. S3*A*) and recombinant SIK2 (Fig. S3*B*) on recombinant HDAC4. Recombinant human MST3, human MST3b, and mouse MST3 could phosphorylate recombinant human SIK1 (Fig. 4*F*) and SIK2 (Fig. 4*G*). Compared with GFP, human MST1, MST2, MST3, MST4, and MST5 immunoprecipitated from HEK cells could phosphorylate recombinant SIK3, although the apparent activity of MST4 was weaker than those of the other four (Fig. 4*H*).

Recombinant SIK3 could be phosphorylated at T221 by recombinant MST1, MST2, and MST3 strongly and MST4 and MST5 weakly (Fig. 7B in the companion article). Recombinant AMPK could be phosphorylated by MST3 strongly and other MSTs weakly (Fig. 7B in the companion

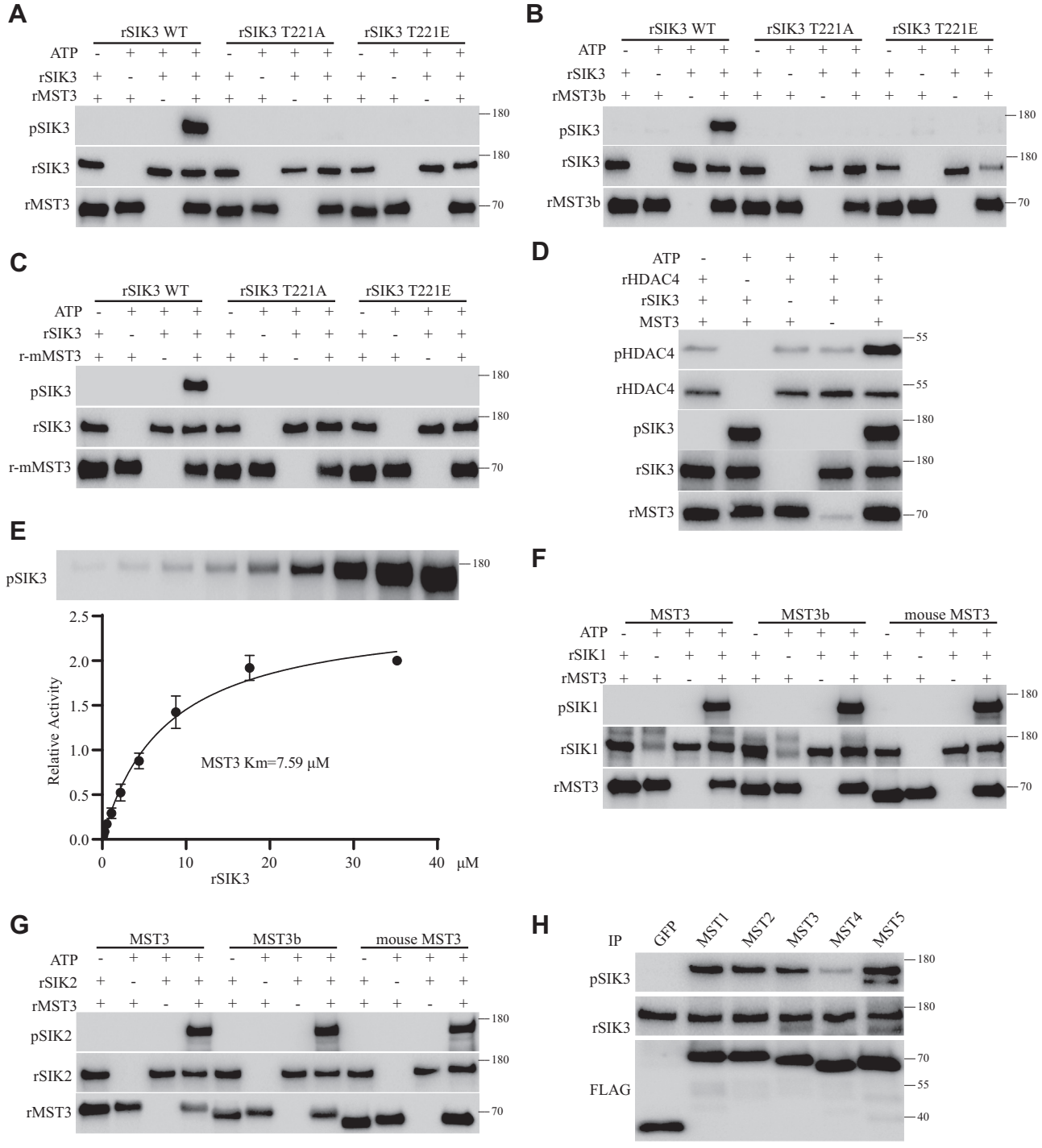

Figure 4. Phosphorylation of SIK3-T221 by recombinant MST3 *in vitro*. All experiments in this figure except that in H were performed with recombinant proteins expressed in *Escherichia coli* (Fig. S7 in the companion article). rSIK3 WT, rSIK3 T221A, and rSIK3 T221E were SIK3 59 to 558 WT and its mutant forms. rMST3 was recombinant human MST3 protein expressed in *E. coli*. MST3b is human MST3b. mMST3 is mouse MST3. rHDAC4 is recombinant human HDAC4 400 to 655. pSIK3 represents SIK3 phosphorylated at T221, whereas pHDAC4 represents HDAC4 phosphorylated at S632. *A*, recombinant human MST3 protein phosphorylated T221 of recombinant SIK3 (rSIK3) but not T221A or T221E mutants of SIK3. *B*, recombinant human MST3b protein phosphorylated rSIK3 at T221 but not its T221A or T221E mutants. *C*, recombinant mouse MST3 protein (r-mMST3) phosphorylated rSIK3 at T221 but not its T221A or T221E mutants. *D*, HDAC4 is a known target for SIK3. Phosphorylation of recombinant HDAC4 by rSIK3 was enhanced by recombinant MST3. Phosphorylation reactions were 1 h at 37 °C with a final concentration of 1 mM ATP. HDAC4 phosphorylation was detected by an anti–phospho-HDAC4 antibody. *E*, the Michaelis–Menten constant of MST3 on SIK3. About 0.2 μg rMST3 was incubated with the rSIK3 substrate of different concentrations at 37 °C for 30 min. Results from Western analysis were quantified by the ImageJ software, and the Michaelis–Menten constant (K_m) was calculated by the GraphPad software. *F*, recombinant SIK1 could be phosphorylated at T182 by recombinant human MST3, human MST3b, and mouse MST3. *G*, recombinant SIK2 could be phosphorylated at T175 by recombinant human MST3, human MST3b, and mouse MST3. *H*, FLAG-tagged GFP and human MST1 to MST5 were individually expressed in HEK cells and immunoprecipitated by the anti-FLAG antibody. Immunoprecipitated GFP did not phosphorylate rSIK3. SIK3-T221 was phosphorylated strongly by immunoprecipitated MST1, MST2, MST3, and MST5 and weakly by immunoprecipitated MST4. HDAC4, histone deacetylase 4; HEK, human embryonic kidney cell; MST3, mammalian sterile 20–like kinase 3; SIK3, salt-inducible kinase 3; T221, threonine 221.

article). The activities of MSTs immunoprecipitated from HEK cells (Fig. 4*H*) did not correlate exactly in strength with those of recombinant MSTs (Fig. 7B in the companion article), which did not rule out the possibility of proteins associated with the immunoprecipitated MSTs.

Phosphorylation of AMPKα by MSTs

Although LKB1 was reported to phosphorylate all ARKs (36), CaMKK2 could only phosphorylate AMPKα T172 but not SIK3-T221 or other ARKs (50). *A priori*, it is unclear whether a kinase for one ARK is also a kinase for other ARKs.

SIK3 is similar in sequence to the α subunit of AMPK. We therefore investigated whether MST3 (and other MSTs) could phosphorylate AMPK α1 and α2, at T183 in α1 and T172 in α2, which are equivalent to T221 of SIK3. When a plasmid expressing a FLAG-tagged form of human MST3 was transfected into HEK cells, increasing amounts of the plasmid led to increasing MST3 expression and increasing AMPKα-T172 phosphorylation (Fig. 5*A*). We generated HEK cell lines with either the Lkb1 gene or the Mst3 gene deleted. When the FLAG-tagged human MST3 was expressed in Mst3 knockout lines (Figs. S4*A* and 4*B*), increasing amounts of MST3 led to increasing AMPKα-T172 phosphorylation. When the FLAG-tagged human MST3 was expressed in Lkb1 knockout lines (Fig. 5*B*), increasing amounts of MST3 also led to increasing AMPKα-T172 phosphorylation. These results suggest that MST3 could increase AMPKα-T172 phosphorylation independent of the endogenous LKB1 in HEK cells.

When expressed in HEK cells, MST3 WT and MST3 T178E increased AMPKα T172 phosphorylation, whereas MST3 T178A and MST3 K53R did not (Fig. 5*C*). MST3 WT and MST3 T178E immunoprecipitated from HEK cells phosphorylated recombinant AMPKα1-T183, whereas MST3 (WT, T178A, T178E, or K53R) immunoprecipitated from HEK cells did not phosphorylate T183A mutant of AMPKα1 (Fig. 5*D*).

To test for the possibility of direct phosphorylation of AMPKα1-T183 by MST3, we expressed their WT and mutant forms as recombinant proteins in *E. coli*. Recombinant MST3 WT, but not recombinant MST3 T178A or MST3 T178E, directly phosphorylated T183 of recombinant AMPKα1 (Fig. 5*E*). Recombinant MST3 (WT, T178A, T178E, or K53R) did not phosphorylate recombinant AMPKα1 with the T183A or the T183E mutation (Fig. 5*E*). These results demonstrate that MST3 directly phosphorylate T183 of AMPKα1.

Recombinant human MST3, human MST3b, and mouse MST3 all could phosphorylate recombinant AMPKα1-T183 (Fig. 5*F*).

To investigate the enzymatic kinetics of MST3 on AMPKα1, we measured the Michaelis–Menten constant of MTS3 (Fig. 5*G*). We determined the Michaelis–Menten constant of MST3 phosphorylation of AMPKα1 by incubating the same concentration of recombinant MST3 with increasing concentrations of the recombinant AMPKα1 substrate. The Michaelis–Menten constant of MST3 phosphorylation of AMPKα1 was found to be 15.72 μM (Fig. 5*G*).

Recombinant AMPKα1 T183 could not be phosphorylated by FLAG-tagged GFP immunoprecipitated from HEK cells but was phosphorylated strongly by MSTs (especially 1 and 2) immunoprecipitated from HEK cells. Under the same conditions, immunoprecipitated MSTs were stronger than immunoprecipitated LKB1 in phosphorylating recombinant AMPKα1 at T183 (Fig. 5*H*) or SIK3 at T221 (Fig. 3*D*).

T183 of recombinant AMPKα1 was strongly phosphorylated by recombinant MST1, MST2, MST3, MST4, and MST5 generated from *E. coli*, though not by recombinant vaccinia-related kinase 1 from *E. coli* (Fig. 5*I*).

To investigate whether MST3 regulates the catalytic activity of AMPKα1, we used acetyl-coenzyme A carboxylase 1 (ACC1), a known substrate for AMPKα (6, 7) and an important enzyme for lipid metabolism (59). Recombinant ACC1 was phosphorylated by FLAG-tagged AMPKα1 immunoprecipitated from HEK cells but not by phosphatase-treated FLAG-tagged AMPKα1 immunoprecipitated from HEK cells (Fig. S4*C*). ACC1 was phosphorylated by WT and T183E forms of AMPKα1 immunoprecipitated from HEK cells (Fig. S4*D*). Recombinant ACC1 was phosphorylated by recombinant AMPKα1 T183E but not by recombinant AMPKα1 WT or T183A (Fig. 4*E*). These results indicate that phosphorylation of AMPKα1 at T183A is important for its direct phosphorylation of ACC1. Recombinant MST3 phosphorylated recombinant AMPKα1 for 1 h at 37 °C in the presence of ATP. T183-phosphorylated or T183-nonphosphorylated recombinant AMPKα1 precipitated from this reaction was then incubated with recombinant ACC1. ACC1 could be phosphorylated strongly by AMPKα1 previously treated with MST3 (Fig. 5*J*). These results demonstrate that MST3 directly phosphorylates AMPKα1 at T183 and increases the catalytic activity of AMPKα1 on its substrate.

We also investigated the effect of MST3 on phosphorylation of the equivalent site T172 in AMPKα2 (Fig. S4, *F–I*). Recombinant AMPKα2 WT but not its T172A mutant could be phosphorylated at T172 by FLAG-tagged MST3 immunoprecipitated from HEK cells (Fig. S4*F*). Recombinant AMPKα2 WT but not its T172A or T172E mutant could be phosphorylated at T172 by recombinant MST3 (Fig. S4*G*). Recombinant AMPKα2 could be phosphorylated at T172 by recombinant human MST3, human MST3b, and mouse MST3 (Fig. S4*H*). The Michaelis–Menten constant of human MST3 on AMPKα2 was determined to be 19.87 μM (Fig. S4*I*). Thus, MST3 could phosphorylate AMPKα1 and AMPKα2.

In summary, we have provided evidence that SIK1, SIK2, SIK3, AMPKα1, and AMPKα2 can be phosphorylated by MST3 *in vitro*. More discussions are provided in the companion article.

Experimental procedures

Reagents

The following antibodies were used: anti–phospho-T172-AMPKα2 (catalog no.: 50081), anti-LKB1 (catalog no.: 3047), anti-AMPKα (catalog no.: 2535), anti–phospho-S79-ACC1 (catalog no.: 3661), anti-MST3 (catalog no.: 3723), anti–phospho-S632-HDAC4 (catalog no.: 3424), anti–phospho-MARK family (activation loop) (catalog no.: 4836) were from

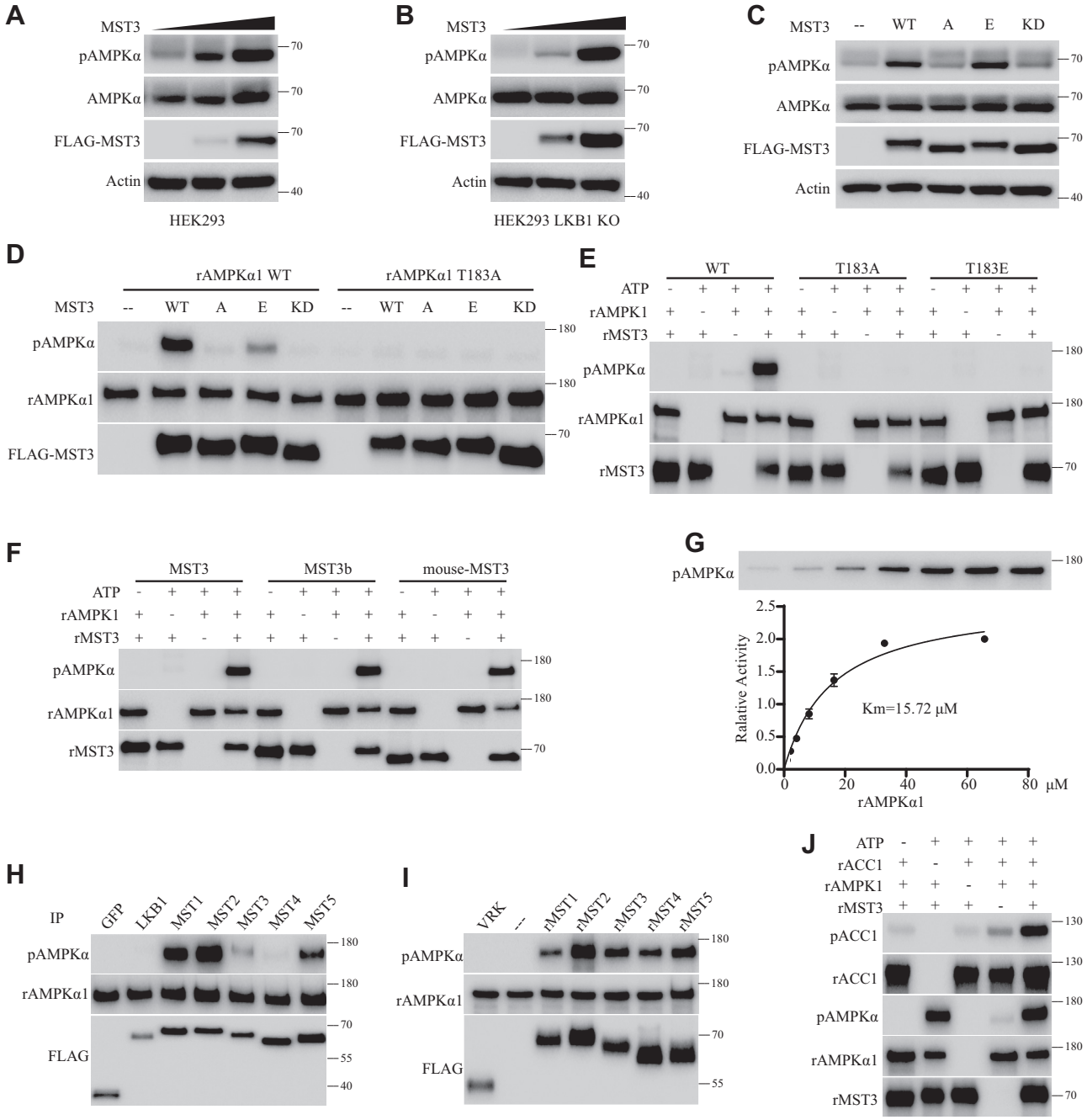

Figure 5. Phosphorylation of AMPKα1-T183 by MSTs *in vivo* and *in vitro*. Experiments in *A*, *B*, and *C* were carried out in HEK cells treated with 200 nM okadaic acid (OA) for 1 h before lysis and analysis with an anti–phospho-AMPK-T172 antibody. Experiments in *D* and *H* were carried out with MSTs immunoprecipitated from HEK cells. Experiments in *E* to *G* and *J* were carried out with recombinant proteins. *A*, HEK293T cells were transfected with a plasmid expressing the FLAG-tagged human MST3 and cultured for 24 h. Cells were treated with 200 nM OA for 1 h before lysis and analysis with an anti–phospho-AMPK-T172 antibody. Increasing amounts of MST3 led to increasing phosphorylation of AMPKα at T172. *B*, we generated an HEK293 cell line with its LKB1 gene deleted (LKB1 KO). The LKB1 KO HEK cell line was transfected with the plasmid expressing the FLAG-tagged MST3. Increasing amounts of MST3 expression led to increasing AMPKα-T172 phosphorylation, in the absence of LKB1. *C*, FLAG-tagged forms of MST3 WT, MST3 T178A (*A*), MST3 T178E (*E*), and MST3 K53R (KD) were expressed in HEK cells. AMPKα-T172 phosphorylation was increased by MST3 WT and MST3 T178E but not by MST3 T178A and MST3 K53R. *D*, recombinant AMPKα1 was phosphorylated by MST3 WT and MST3 T178E immunoprecipitated from HEK cells but not by MST3 T178A or MST3 K53R immunoprecipitated from HEK cells. Recombinant AMPKα1 with T183A mutation was not phosphorylated by any form of MST3 (WT, T178A, T178E, or K53R) immunoprecipitated from HEK cells. *E*, recombinant AMPKα1 was phosphorylated directly by recombinant MST3. Recombinant AMPKα1 with T183A or T183E mutation was not phosphorylated by recombinant MST3. *F*, recombinant AMPKα1 was phosphorylated at T183 directly by recombinant human MST3, human MST3b, and mouse MST3. *G*, the Michaelis–Menten constant of recombinant MST3 with recombinant AMPKα1 was 15.72 μM. *H*, FLAG-tagged proteins (GFP, LKB1, and MST 1–5) individually expressed in, and immunoprecipitated from, HEK cells were tested for their activities on recombinant AMPKα1. AMPKα1-T183 was phosphorylated strongly by immunoprecipitated MST1 and MST2, moderately by immunoprecipitated MST5 and MST3, and very weakly by immunoprecipitated MST4. All these activities were higher than that of LKB1 (not visible here because of exposure in the same time window already showed strong signals for MST1 and MST2). *I*, recombinant FLAG-tagged proteins were expressed in *Escherichia coli* and purified. While recombinant VRK1 showed no activity, recombinant MST1, MST2, MST3, MST4, and MST5 all showed strong activity in phosphorylating AMPKα1 T183. *J*, recombinant AMPKα1 was incubated with recombinant MST3 for 1 h at 37 °C with a final concentration of 1 mM ATP. MST3 was removed before the supernatant was assayed with recombinant ACC1. Recombinant AMPKα1 could phosphorylate ACC1, and this was increased by prior treatment with recombinant MST3. ACC1, acetyl-coenzyme A carboxylase 1; AMPK, AMP-activated protein kinase; HEK, human embryonic kidney cell; LKB1, liver kinase B1; MST, mammalian sterile 20–like; T172, threonine 172; T183, threonine 183; VRK1, vaccinia-related kinase 1.

Cell Signaling Technology; anti–β-actin (catalog no.: sc-47778) and anti-SIK3 (catalog no.: sc515408) were from Santa Cruz Biotechnology; anti–phospho-SIK family (activation loop) (catalog no.: ab199474), anti-SIK1 (catalog no.: ab64428), anti-SIK2 (catalog no.: ab53423) antibodies and okadaic acid (catalog no.: ab141831) were from Abcam Biotechnology; anti-FLAG M2 horseradish peroxidase conjugated (catalog no.: A8592), phosphatase inhibitor cocktail 2 (catalog no.: P5726), phosphatase inhibitor cocktail 3 (catalog no.: P0044), protease inhibitor cocktail tablets (catalog no.: 04693132001) were from Sigma; anti–phospho-BRSK family (activation loop) (catalog no.: spc-927), anti–phospho-NUAK family (activation loop) (catalog no.: spc-1036) were from Stressmarq Biosciences, Inc.

Transfection and immunoprecipitation

cDNAs were cloned into the pcDNA 3.1 vector with indicated tags at the N terminus. Cells were cultured in Dulbecco's modified Eagle's medium (Gibco) with 10% fetal bovine serum (Gibco) and 1% penicillin/streptomycin (Gibco) with standard supplements. HEK293T cells were transfected with Lipofectamine 3000 reagent (Thermo Fisher Scientific) according to the manufacturer's instructions and harvested 24 to 36 h after transfection. Cells were collected and lysed on ice with lysis buffer (25 mM Tris–HCl [pH 7.5], 150 mM NaCl, 5 mM $MgCl_2$, 0.3% Chaps, 1 mM DTT, 1× protease inhibitor cocktail, 1× phosphatase inhibitor II, and 1× phosphatase inhibitor III). Cell lysates were centrifugated at 14,000 rpm for 30 min at 4 °C. Lysates were incubated with 25 μl anti-FLAG Magnetic Agarose slurry balanced for 1 h. After being washed with lysis buffer three times, beads were washed with 0.5 mg/ml 3× FLAG Peptide in buffer A at room temperature and stored at −80 °C.

Expression and purification of recombinant proteins

cDNAs were cloned into the pET-28a vector with indicated tags. Plasmids were transformed into *E. coli* BL21 cells and induced with 0.5 mM IPTG at 18 °C for 16 h. Cells were harvested and suspended in Ni binding buffer (300 mM NaCl, 20 mM Tris–HCl, pH 7.5) supplemented with protease inhibitors. Cells were lysed by sonication and centrifuged at 14,000 rpm for 30 min. Supernatant was filtered by 0.45 μm filter and purified to 90% purity by tandem Ni^{2+} and dextran affinity column. Pooled elution fractions were stained by Coomassie blue and stored at −80 °C. Some are shown in Figure S7 of the companion article.

Recombinant SIK3 was generated as a fusion protein as MBP-tobacco etch virus (TEV)-3x FLAG-SIK3 59-558-TEV-GFP-8xHis tag. When it was used as a substrate for upstream kinases, it was used as such. When it was tested as a kinase itself (Fig. S3), it was cleaved at TEV sites and releases as SIK3 59 to 558 without the other proteins or tags.

In vitro *kinase assay*

Purified fractions (10 μl) or recombinant kinases (0.5 μg) were incubated with 1 μg substrates at 37 °C for 1 h in buffer A (20 mM Hepes, 10 mM KCl, 1.5 mM $MgCl_2$, 1 mM EDTA, 1 mM EGTA, 1 mM DTT, 1× protease inhibitor cocktail, 1× phosphatase inhibitor II, and 1× phosphatase inhibitor III) with a final concentration of 1 mM ATP (pH 7.5) in a total volume of 20 μl. The reaction was terminated by heating at 95 °C with the protein loading buffer and analyzed by immunoblotting.

Calculation of Michaelis–Menten constant

About 0.2 μg of each recombinant kinase was incubated with the substrate at multiple concentrations at 37 °C for 30 min in buffer A supplemented with protease inhibitors and phosphatase inhibitors. Reactions were terminated by heating at 95 °C with the protein loading buffer and followed by Western analysis. Western blots were quantitated with ImageJ software, and the K_m was calculated by GraphPad software.

Purification of MST3 from HEK293T cells

We applied 500 ml HEK293T cell lysates (at a concentration of 10 mg/ml) to six sequentially connected chromatography steps as diagramed in Figure 2*A*, with Western analysis results shown in Figure 2*A*. The purification was performed at 4 °C with an AKTA Purifier 10 FPLC system (GE Healthcare). Cell lysates were loaded onto two tandem-connected 5 ml HiTrap SP HP columns pre-equilibrated with buffer A. Columns were washed with 5 CV of buffer A and eluted with a linear gradient of 20 CV buffer A from 0 to 600 mM NaCl. About 20 fractions were collected, and aliquots of 0.5 ml of each fraction were dialyzed against buffer A and followed by *in vitro* SIK3 phosphorylation assay. Active fractions from SP HP columns (fraction 7, 180 mM NaCl) (Fig. 3*A*) were pooled and loaded on two tandem-connected 5 ml HiTrap Heparin HP columns, which were washed with 5 CV of buffer A and eluted with a linear gradient of 0 to 600 mM NaCl in 20 CV buffer A. Fractions were dialyzed and assayed. Active fractions (9, 10, and 11; 270–300 mM NaCl) from the heparin column (Fig. 3*B*) were loaded on two tandem-connected 1 ml HiTrap Q HP columns, which were washed with 5 CV of buffer A and eluted with a linear gradient of 0 to 600 mM NaCl in 20 CV buffer A. Active fractions (10 and 11; 270–300 mM NaCl) from the Q HP column (Fig. 3*C*) were pooled and loaded on 1 ml HAP column (Bio-Rad), eluted with a linear gradient of K_2PO_4 buffer from 0 to 300 mM. Active fractions (10 and 11; 135–150 mM K_2PO_4) from the HAP column (Fig. 3*D*) were pooled and concentrated to 0.5 ml and loaded onto a Superdex 75 10/300 GL column and eluted with 200 mM NaCl in buffer A. The resulting fractions were dialyzed and assayed for SIK3 phosphorylation activity. Active fractions (13 and 14; 360–390 mM NaCl) from Superdex 75 10/300 GL column (Fig. 3*E*) were pooled, loaded on a Mono S 5/50 GL column, and eluted with a linear gradient of 20 CV buffer A from 0 to 600 mM NaCl. Fractions were dialyzed against buffer A, and each was assayed for activity and analyzed by silver staining. All procedures were approved by Center for Innovative Biomedical Resources Animal Research Committee.

Data availability

All data are contained in the article.

Supporting information—This article contains supporting information (four supporting figures).

Acknowledgments—We are grateful to Peking-Tsinghua Center for Life Sciences, Center for Innovative Biomedical Resources, and Changping Laboratory for support.

Author contributions—Y. R. and Y. L. conceptualization; Y. L. methodology; Y. L., T. V. W., Y. C., and S. G. validation; Y. R., Y. K., T. V. W., and S. G. formal analysis; Y. L., T. V. W., Y. C., and S. G. investigation; Y. R. and Y. L. writing–original draft; Y. L. and T. V. W. writing–review and editing; Y. L., T. V. W., and Y. C. visualization; Y. R. supervision; Y. R. funding acquisition.

Conflict of interest—The authors declare that they have no conflicts of interest with the contents of this article.

Abbreviations—The abbreviations used are: ACC1, acetyl-coenzyme A carboxylase 1; AMPK, AMP-activated protein kinase; ARK, AMPK-related kinase; CaMKK2, Ca^{2+}/calmodulin-dependent protein kinase kinase 2; cDNA, complementary DNA; CV, column volume; HAP, hydroxyapatite; HDAC4, histone deacetylase 4; HEK, human embryonic kidney cell; LKB1, liver kinase B1; MST, mammalian sterile 20–like; MST3, mammalian sterile 20–like kinase 3; NaCl, sodium chloride; Q HP, Q sepharose high performance column; SIK3, salt-inducible kinase 3; SP HP, SP sepharose high performance column; T172, threonine 172; T183, threonine 183; T221, threonine 221; TEV, tobacco etch virus.

References

1. Beg, Z. H., Allmann, D. W., and Gibson, D. M. (1973) Modulation of 3-hydroxy-3-methylglutaryl coenzyme A reductase activity with cAMP and wth protein fractions of rat liver cytosol. *Biochem. Biophys. Res. Commun.* **54**, 1362–1369
2. Carlson, C. A., and Kim, K. H. (1973) Regulation of hepatic acetyl coenzyme A carboxylase by phosphorylation and dephosphorylation. *J. Biol. Chem.* **248**, 378–380
3. Ingebritsen, T. S., Lee, H. S., Parker, R. A., and Gibson, D. M. (1978) Reversible modulation of activities of both liver microsomal hydroxymethylglutaryl coenzyme a reductase and its inactivating enzyme-evidence for regulation by phosphorylation-dephosphorylation. *Biochem. Biophys. Res. Commun.* **81**, 1268–1277
4. Yeh, L. A., Lee, K. H., and Kim, K. H. (1980) Regulation of rat liver acetyl-CoA carboxylase. Regulation of phosphorylation and inactivation of acetyl-CoA carboxylase by the adenylate energy charge. *J. Biol. Chem.* **255**, 2308–2314
5. Ferrer, A., Caelles, C., Massot, N., and Hegardt, F. G. (1985) Activation of rat liver cytosolic 3-hydroxy-3-methylglutaryl coenzyme A reductase kinase by adenosine 5'-monophosphate. *Biochem. Biophys. Res. Commun.* **132**, 497–504
6. Carling, D., Zammit, V. A., and Hardie, D. G. (1987) A common bicyclic protein kinase cascade inactivates the regulatory enzymes of fatty acid and cholesterol biosynthesis. *FEBS Lett.* **223**, 217–222
7. Munday, M. R., Campbell, D. G., Carling, D., and Hardie, D. G. (1988) Identification by amino acid sequencing of three major regulatory phosphorylation sites on rat acetyl-CoA carboxylase. *Eur. J. Biochem.* **175**, 331–338
8. Carling, D., Clarke, P. R., Zammit, V. A., and Hardie, D. G. (1989) Purification and characterization of the AMP-activated protein kinase. Copurification of acetyl-CoA carboxylase kinase and 3-hydroxy-3-methylglutaryl-CoA reductase kinase activities. *Eur. J. Biochem.* **186**, 129–136
9. Hardie, D. G. (2014) AMP-activated protein kinase: Maintaining energy homeostasis at the cellular and whole-body levels. *Annu. Rev. Nutr.* **34**, 31–55
10. Lopez, M., Nogueiras, R., Tena-Sempere, M., and Dieguez, C. (2016) Hypothalamic AMPK: A canonical regulator of whole-body energy balance. *Nat. Rev. Endocrinol.* **12**, 421–432
11. Hardie, D. G., Schaffer, B. E., and Brunet, A. (2016) AMPK: An energy-sensing pathway with multiple inputs and outputs. *Trends Cell Biol.* **26**, 190–201
12. Herzig, S., and Shaw, R. J. (2018) AMPK: Guardian of metabolism and mitochondrial homeostasis. *Nat. Rev. Mol. Cell Biol.* **19**, 121–135
13. Hsu, C.-. C., Zhang, X., Wang, G., Zhang, W., Cai, Z., Pan, B.-S., Gu, H., Xu, C., Jin, G., Xu, X., Manne, R. K., Jin, Y., Yan, W., Shao, J., Chen, T., *et al.* (2021) Inositol serves as a natural inhibitor of mitochondrial fission by directly targeting AMPK. *Mol. Cell* **81**, 3803–3819
14. Steinberg, G. R., Dandapani, M., and Hardie, D. G. (2013) AMPK: Mediating the metabolic effects of salicylate-based drugs? *Trends Endocrinol. Metab.* **24**, 481–487
15. Carling, D. (2017) AMPK signalling in health and disease. *Curr. Opin. Cell Biol.* **45**, 31–37
16. Day, E. A., Ford, R. J., and Steinberg, G. R. (2017) AMPK as a therapeutic target for treating metabolic diseases. *Trends Endocrinol. Metab.* **28**, 545–560
17. Russell, F. M., and Hardie, D. G. (2021) AMP-activated protein kinase: Do we need activators or inhibitors to treat or prevent cancer? *Int. J. Mol. Sci.* **22**, 186
18. Davies, S. P., Hawley, S. A., Woods, A., Carling, D., Haystead, T. A., and Hardie, D. G. (1994) Purification of the AMPK-activated protein kinase on ATP-gamma Sepharose and analysis of its subunit structure. *Eur. J. Biochem.* **223**, 351–357
19. Mitchelhill, K. I., Stapleton, D., Gao, G., House, C., Michel, B., Katsis, F., Witters, L. A., and Kemp, B. E. (1994) Mammalian AMP-activated protein kinase shares structural and functional homology with the catalytic domain of yeast Snf1 protein kinase. *J. Biol. Chem.* **269**, 2361–2364
20. Michell, B., Stapleton, D., Mitchelhill, K. I., House, C. M., Katsis, F., Witters, L. A., and Kemp, B. E. (1996) Isoform-specific purification and substrate specificity of the 5'-AMP-activated protein kinase. *J. Biol. Chem.* **271**, 28445–28450
21. Carling, D., Aguan, K., Woods, A., Verhoeven, A. J. M., Beri, R. K., Brennan, C. H., Sidebottom, C., Davison, M. D., and Scott, J. (1994) Mammalian AMP-activated protein kinase is homologous to yeast and plant protein kinases involved in the regulation of carbon metabolism. *J. Biol. Chem.* **269**, 11442–11448
22. Gao, G., Widmer, J., Stapleton, D., Teh, T., Cox, T., Kemp, B. E., and Witters, L. A. (1995) Catalytic subunits of the porcine and rat 5'-AMP-activated protein kinase are members of the SNF1 protein kinase family. *Biochim. Biophys. Acta* **1266**, 73–82
23. Stapleton, D., Gao, G., Michell, B. J., Widmer, J., Mitchelhill, K., Teh, T., House, C. M., Witters, L. A., and Kemp, B. E. (1994) Mammalian 5'-AMP-activated protein-kinase noncatalytic subunits are homologs of proteins that interact with yeast Snf1 protein-kinase. *J. Biol. Chem.* **269**, 29343–29346
24. Gao, G., Fernandez, C. S., Stapleton, D., Auster, A. S., Widmer, J., Dyck, J. R., Kemp, B. E., and Witters, L. A. (1996) Non-catalytic beta- and gamma-subunit isoforms of the 5'-AMP-activated protein kinase. *J. Biol. Chem.* **271**, 8675–8681
25. Woods, A., Cheung, P. C., Smith, F. C., Davison, M. D., Scott, J., Beri, R. K., and Carling, D. (1996) Characterization of AMP-activated protein kinase beta and gamma subunits - assembly of the heterotrimeric complex *in vitro*. *J. Biol. Chem.* **271**, 10282–10290
26. Stapleton, D., Mitchelhill, K. I., Gao, G., Widmer, J., Michell, B. J., The, T., House, C. M., Fernandez, C. S., Cox, T., Witters, L. A., and Kemp, B. E. (1996) Mammalian AMP-activated protein kinase subfamily. *J. Biol. Chem.* **271**, 611–614
27. Dyck, J. R. B., Gao, G., Widmer, J., Stapleton, D., Fernandez, C. S., Kemp, B. E., and Witter, L. A. (1996) Regulation of 5-'AMP-activated protein

kinase activity by the noncatalytic beta and gamma subunits. *J. Biol. Chem.* **271**, 17798–17803
28. Woods, A., Salt, I., Scott, J., Hardie, D. G., and Carling, D. (1996) The alpha1 and alpha2 isoforms of the AMP-activated protein kinase have similar activities in rat liver but exhibit differences in substrate specificity *in vitro*. *FEBS Lett.* **397**, 347–351
29. Hawley, S. A., Davison, M., Woods, M., Davies, S. P., Beri, R. K., Carling, D., and Hardie, D. G. (1996) Characterization of the AMP-activated protein kinase kinase from rat liver and identification of threonine 172 as the major site at which it phosphorylates AMP-activated protein kinase. *J. Biol. Chem.* **271**, 27879–27887
30. Hemminki, A., Markie, D., Tomlinson, I., Avizienyte, E., Roth, S., Loukola, A., Bignell, G., Warren, W., Aminoff, M., Höglund, P., Järvinen, H., Kristo, P., Pelin, K., Ridanpää, M., Salovaara, R., *et al.* (1998) A serine/threonine kinase gene defective in Peutz-Jeghers syndrome. *Nature* **391**, 184–187
31. Hawley, S. A., Boudeau, J., Reid, J. L., Mustard, K. J., Udd, L., Mäkelä, T. P., Alessi, D. R., and Hardie, D. G. (2003) Complexes between the LKB1 tumor suppressor, STRAD alpha/beta and MO25 alpha/beta are upstream kinases in the AMP-activated protein kinase cascade. *J. Biol.* **2**, 28
32. Woods, A., Johnstone, S. R., Dickerson, K., Leiper, F. C., Fryer, L. G. D., Neumann, D., Schlattner, U., Wallimann, T., Carlson, M., and Carling, D. (2003) LKB1 is the upstream kinase in the AMP-activated protein kinase cascade. *Curr. Biol.* **13**, 2004–2008
33. Sutherland, C. M., Hawley, S. A., McCartney, R. R., Leech, A., Stark, M. J. R., Schmidt, M. C., and Hardie, D. G. (2003) Elm1p is one of three upstream kinases for the Saccharomyces cerevisiae SNF1 complex. *Curr. Biol.* **13**, 1299–1305
34. Hong, S.-P., Leiper, F. C., Woods, A., Carling, D., and Carlson, M. (2003) Activation of yeast Snf1 and mammalian AMP-activated protein kinase by upstream kinases. *Proc. Natl. Acad. Sci. U. S. A.* **100**, 8839–8843
35. Shaw, R. J., Kosmatka, M., Bardeesy, N., Hurley, R. L., Witters, L. A., DePinho, R. A., and Cantley, L. C. (2004) The tumor suppressor LKB1 kinase directly activates AMP-activated kinase and regulates apoptosis in response to energy stress. *Proc. Natl. Acad. Sci. U. S. A.* **101**, 3329–3335
36. Lizcano, J. M., Göransson, O., Toth, R., Deak, M., Morrice, N. A., Boudeau, J., Hawley, S. A., Udd, L., Mäkelä, T. P., Hardie, D. G., and Alessi, D. R. (2004) LKB1 is a master kinase that activates 13 kinases of the AMPK subfamily, including MARK/PAR-1. *EMBO J.* **23**, 833–843
37. Sakamoto, K., McCarthy, A., Smith, D., Green, K. A., Hardie, D. G., Ashworth, A., and Alessi, D. R. (2005) Deficiency of LKB1 in skeletal muscle prevents AMPK activation and glucose uptake during contraction. *EMBO J.* **24**, 1810–1820
38. Shaw, R. J., Lamia, K. A., Vasquez, D., Koo, S.-H., Bardeesy, N., DePinho, R. A., Montminy, M., and Cantley, L. C. (2005) The kinase LKB1 mediates glucose homeostasis in liver and therapeutic effects of metformin. *Science* **310**, 1642–1646
39. Hawley, S. A., Pan, D. A., Mustard, K. J., Ross, L., Bain, J., Edelman, A. M., Frenguelli, B. G., and Hardie, D. G. (2005) Calmodulin-dependent protein kinase kinase-beta is an alternative upstream kinase for AMP-activated protein kinase. *Cell Metab* **2**, 9–19
40. Hurley, R. L., Anderson, K. A., Franzone, J. M., Kemp, B. E., Means, A. R., and Witters, L. A. (2005) The Ca2+/calmodulin-dependent protein kinase kinases are AMP-activated protein kinase kinases. *J. Biol. Chem.* **280**, 29060–29066
41. Woods, A., Dickerson, K., Heath, R., Hong, S.-P., Momcilovic, M., Johnstone, S. R., Carlson, M., and Carling, D. (2005) Ca2+/calmodulin-dependent protein kinase kinase-beta acts upstream of AMP-activated protein kinase in mammalian cells. *Cell Metab.* **2**, 21–33
42. Anderson, K. A., Ribar, T. J., Lin, F., Noeldner, P. K., Green, M. F., Muehlbauer, M. J., Witters, L. A., Kemp, B. E., and Means, A. R. (2008) Hypothalamic CaMKK2 contributes to the regulation of energy balance. *Cell Metab.* **7**, 377–388
43. Momcilovic, M., Hong, S. P., and Carlson, M. (2006) Mammalian TAK1 activates Snf1 protein kinase in yeast and phosphorylates AMP-activated protein kinase *in vitro*. *J. Biol. Chem.* **281**, 25336–25343
44. Xie, M., Zhang, D., Dyck, J. R., Li, Y., Zhang, H., Morishima, M., Mann, D. L., Taffet, G. E., Baldini, A., Khoury, D. S., and Schneider, M. D. (2006) A pivotal role for endogenous TGF-beta-activated kinase-1 in the LKB1/AMP-activated protein kinase energy-sensor pathway. *Proc. Natl. Acad. Sci. U. S. A.* **103**, 17378–17383
45. Scholz, R., Sidler, C. L., Thali, R. F., Winssinger, N., Cheung, P. C., and Neumann, D. (2010) Autoactivation of transforming growth factor beta-activated kinase 1 Is a sequential bimolecular process. *J. Biol. Chem.* **285**, 25753–25766
46. Neumann, D. (2018) Is TAK1 a direct upstream kinase of AMPK? *Int. J. Mol. Sci.* **19**, 2412
47. Funato, H., Miyoshi, C., Fujiyama, T., Kanda, T., Sato, M., Wang, Z., Ma, J., Nakane, S., Tomita, J., Ikkyu, A., Kakizaki, M., Hotta-Hirashima, N., Kanno, S., Komiya, H., Asano, F., *et al.* (2016) Forward-genetics analysis of sleep in randomly mutagenized mice. *Nature* **539**, 378–383
48. Park, M., Miyoshi, C., Fujiyama, T., Kakizaki, M., Ikkyu, A., Honda, T., Choi, J., Asano, F., Mizuno, S., Takahashi, S., Yanagisawa, M., and Funato, H. (2020) Loss of the conserved PKA sites of SIK1 and SIK2 increases sleep need. *Sci. Rep.* **10**, 8676
49. preprint Li, Y., Zhou, E., Liu, Y., Yu, J., Yang, J., Li, C., Cui, Y., Wang, T., Li, C., Liu, Z., and Rao, Y. (2021) Sleep need, the key regulator of sleep homeostasis, is indicated and controlled by phosphorylation of threonine 221 in salt inducible kinase 3. *bioRxiv*. https://doi.org/10.1101/2021.11.06.467421
50. Fogarty, S., Hawley, S. A., Green, K. A., Saner, N., Mustard, K. J., and Hardie, D. G. (2010) Calmodulin-dependent protein kinase kinase-beta activates AMPK without forming a stable complex: Synergistic effects of Ca2+ and AMP. *Biochem. J.* **426**, 109–118
51. Dan, I., Watanabe, N. M., and Kusumi, A. (2001) The Ste20 group kinases as regulators of MAP kinase cascades. *Trends Cell Biol.* **11**, 220–230
52. Rawat, S. J., and Chernoff, J. (2015) Regulation of mammalian Ste20 (Mst) kinases. *Trends Biochem. Sci.* **40**, 149–156
53. Pombo, C. M., Iglesias, C., Sartages, M., and Zalvide, J. B. (2019) MST kinases and metabolism. *Endocrinology* **160**, 1111–1118
54. Gordon, J., Hwang, J., Carrier, K. J., Jones, C. A., Kern, Q. L., Moreno, C. S., Karas, R. H., and Pallas, D. C. (2011) Protein phosphatase 2a (PP2A) binds within the oligomerization domain of striatin and regulates the phosphorylation and activation of the mammalian Ste20-Like kinase Mst3. *BMC Biochem.* **12**, 54
55. Zhou, T.-H., Ling, K., Guo, J., Zhou, H., Wu, Y.-L., Jing, Q., Ma, L., and Pei, G. (2000) Identification of a human brain-specific isoform of mammalian STE20-like kinase 3 that is regulated by cAMP-dependent protein kinase. *J. Biol. Chem.* **275**, 2513–2519
56. van der Linden, A. M., Nolan, K. M., and Sengupta, P. (2007) KIN-29SIK regulates chemoreceptor gene expression via an MEF2 transcription factor and a class IIHDAC. *EMBO J.* **26**, 358–370
57. Berdeaux, R., Goebel, N., Banaszynski, L., Takemori, H., Wandless, T., Shelton, G. D., and Montminy, M. (2007) SIK1 is a class II HDAC kinase that promotes survival of skeletal myocytes. *Nat. Med.* **13**, 597–603
58. Fujii, S., Emery, P., and Amrein, H. (2017) SIK3-HDAC4 signaling regulates Drosophila circadian male sex drive rhythm via modulating the DN1 clock neurons. *Proc. Natl. Acad. Sci. U. S. A.* **114**, E6669–E6677
59. Abu-Elheiga, L., Matzuk, M. M., Abo-Hashema, K. A. H., and Wakil, S. J. (2001) Continuous fatty acid oxidation and reduced fat storage in mice lacking acetyl-CoA carboxylase 2. *Science* **291**, 2613–2616